ISSN 1070-3632, Russian Journal of General Chemistry, 2010, Vol. 80, No. 3, pp. 591–603. © Pleiades Publishing, Ltd., 2010.
Original Russian Text © R.B. Morgunov, Dmitriev, 2010, published in Rossiiskii Khimicheskii Zhurnal, 2010, Vol. 53, No. 2, pp. 36–46.

Ferromagnetic Semiconductor Nanostructures— Future Spintronics

R. B. Morgunov and A. I. Dmitriev

Semenov Institute of Chemical Physics Problems, Russian Academy of Sciences, Prosp. Akad. Semenova 1, Chernogolovka, Moscow Oblast, 142432 Russia
e-mail: morgunov20062006@yandex.ru

Received January 10, 2009

Abstract—The review analyzes and summarizes the principal results of research on the magnetic properties of ferromagnetic semiconductor nanostructures. These materials possess unique physical properties, which attracts great attention both from the scintific and practical viewpoints. The review shows that group $A_{II}B_{VI}$ and $A_{III}B_{V}$ ferromagnetic semiconductors, as well as group IV elemental semiconductors hold the greatest promise for spintronic applications.

Nanostructuring allows to increase the Curie temperature corresponding to the percolation transition in elemental semiconductors. Approaches to overcoming the principal barrier to spintronics applications of ferromagnetic semiconductors─the necessity of their deep cooling─are considered. Comparison of the magnetic and magnetotransport properties of quasi-one-dimensional $Ge_{1-x}Mn_x$ nanowires with quasi-two-dimensional nanofilms of the same composition reveals an effect of limited size on the ferromagnetic ordering temperature and magnetic resistance.

DOI: 10.1134/S1070363210030400

INTROUCTION

Modern electronics uses semiconductor materials whose functioning is based on electron charge. Enhancing requirements to characteristics of electronic devices prompt demand for search and pracatical implementation of alternative materials based on non-classical principles. Spintronic devices which employ both electron charge and spin may form a basis of future electronics.

Spintronics was first mentioned in 1988 after the discovery of the giant magnetoresistance (GMR) effect [1, 2] (the authors of this discovery were awarded the Nobel Prize in Physics in 2007). The GMR effect is underlain by nonuniform scattering on ferromagnetic impurities of two groups of electrons with spin-up and spin-down orientations. To implement this selection requires that spin-up and spin-down electrons have much different mean free path distances. Such situation takes place is ferromagnetic materials in which 3*d* band splitting induces differentiation in vacant spin-up and spin-down electron state densities. This principle forms the basis of operation of giant and tunnel magnetoresistance devices [3–9].

The progress in the development of information processing means is directly related to the state of data storage technologies. The creation of magnetic random access memory (MRAM) chips belongs to revolutionary achievements in this field [10]. Each cell in MRAM is a nanosized area of a ferromagnetic material and can serve as a memory bit. Information reading in a MRAM is based on the giant or tunnel magnetoresistance effect. A potential difference is applied to control buses of a MRAM (Fig. 1), and, if the magnetization direction of the controlled ferromagnetic

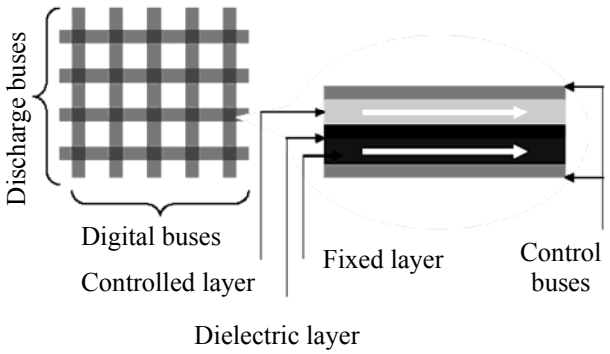

Fig. 1. Scheme of MRAM.

layer coincides of that of the fixed ferromagnetic layer, then the tunnel current runs through the dielectric layer. In the case of opposite magnetizations, the tunnel current is absent. MRAMs override the existing memory types in all respects. At present MRAMs with a capacity of 4 Mbit and a read time of 25 ns are available.

In perspective, massives of ordered ferromagnetic nanowires can be used as MRAMs, provided they have a high Curie temperature. In this case, the density of memory cells can be increased by three orders of magnitude. In [11–14], $Ge_{1-x}Mn_x$ nanowires (x is the atomic fraction of magnetic dopant) ferromagnetic at room temperature were used as functional purpose nanostructures.

Note that spintronics is not limited by the development of logic elements and information storage devices. Spintronics opens up new perspectives in communication means, quantum computing, etc. At present laboratory prototypes of spintronic devices, such as unipolar spin transistors [15] and bipolar spin transistors [16] have already been created.

There are the following requirements to materials for spintronic instruments. First, such materials should be resistant to "normal" environmental effects, i.e. they should preserve their properties at increased (or decreased) humidity, pressure, or temperature. Second, they should be adaptable, specifically allow applying ohmic contacts and combining with modern electronic units. Third, an especially important requirement is associated with the electron spin coherence time. If this time is too short, then spin disorientation leads to a loss of spn information. The use of spin coherence is exemplified by the magnetization precession in Co/Cu multilayers, induced by high-density electric current ($\sim 10^9$ A cm^{-2}) [17, 18]. Forth, materials should be ferromagnetic at room temperature, and charges in them should be highly mobile. Note that no organic and organometallic materials meeting at least partly the above requirements have still been developed. (However, such materials are called functional and invariably associated with spintronics. We consier these pretensions groundless.)

The measurements showed that the spin coherence time at room temperature in semiconductors is several orders of magnitude longer (> 100 ns) than in metals (~0.1–20 ns) that most commonly used in spintronic multilayers [19, 20]. Therefore, "semiconductor" spintronics is more attractive and realistic that "metallic."

At present much effort is focused on the development of diluted magnetic semiconductors (DMS) which are expected to meet all demands made by spintronics. In spite of the gain in spin coherence time, most of the studied DMS materials have quite a low Curie temperature, which hinders practical implementation of the previously discovered spin-dependent transport [21], magneto-optical spin effects [22–24], and electrical manipulation of the Curie temperature and coercive field [25, 26]. This problem can be attacked by passing to DMS nanostructures in which most transition metal dopants are dispersed rather than clustered.

Theoretical Models of Ferromagnetic Ordering in Semiconductors

The unique physical properties of DMS arise from a strong interaction of charge carriers and the magnetic moments of partly filled electronic shells of magnetic atoms and ions. Magnetic ordering affects the mobility of charge carriers, and their concentration, in its turn, much affects magnetic ordering, thus allowing mutually controlling the electronic and magnetic systems of the material.

In metals and their alloys, direct exchange spin coupling between atoms whose magnetic moment is associated with their partly filled electron shells which overlap due to a short interatomic distance in the crystal lattice. The direct exchange coupling in DMS materials cannot induce ferromagnetism, since the distances between neighboring dopant atoms are too long for their electron shells to overlap.

The question whether the ferromagnetic ordering in DMS materials is induced by indirect exchange coupling is still open. A number of theoretical models to explain the origin of DMS ferromagnetism have been developed, such as the Ruderman–Kittel–Kasuya–Yosida (RKKY) [27], double exchange [28], Zener [29, 30], and mean-field theories [31]. None of these theories are universal and are capable of describing the ferromagnetic ordering in an individual DMS group.

The simplest (and the most popular up until recently) phenomenological approach is based on a model taking Zener's *sd* exchange as the initial coupling between the local spin of a magnetic dopant and conduction electrons. The Zener's model consoders two electronic subsystems: the system of collective conduction electrons (*s* electrons) and the

system of localized *d*(*f*) electrons. The Hamiltonian for this model has the form:

$$H = H_M + H_A + H_B,$$

where H_M is the magnetic subsystem Hamiltonian (usually it is taken in the Heizenberg's form $H_M = J_{i,j} S_i S_j$ ($J_{i,j}$ is the exchange integral for the *i*th and *j*th atoms; and S_i, S_j, corresponding spin operators); H_A, the exchange Hamiltonian between conduction electrons and magnetic ion spins; and H_B, Hamiltonian of conduction electrons including single band energy states.

The theoretical results obtained by this model only qualitatively coincide with experimental. For example, the model predicted an increase of the Curie temperature with increasing concentration of admixture ions, which is indeed the case. However, quantitatively, no predictive power was shown. Thus, for example, the calculated Curie temperature T_C, obtained by the Zener's model for $Ga_{1-x}Mn_xAs$ is 300 K, whereas the experimental T_C is no higher than 170 K [32].

At present the ferromagnetic ordering in DMS is explained in terms of the RKKY theory which suggests that localized electrons are incorporated in partly filled *d* and *f* shells, and are coupled via conduction electrons. The contribution of conduction electron spins into the total magnetic moment of a ferromagnetic crystal is low compared with the contribution of localized electrons. However, it is spin-polarized electrons that provide magnetic ordering, since by moving along the crystal they "transfer" spin coupling of transition metal ions.

The Curie temperature predicted by this and any other model should also be dependent on the magnetic dopant concentration, which is consistent with experimental data [35–37]. However, the absolute Curie temperatures predicted for Group IV element DMS materials do not reproduce experiment.

The exchange coupling in (Ga,Mn)As semiconductors cannot be rationalized entirely in terms of a single indirect exchange model [28, 38], even though the Zener's double exchange mechanism [31] well explains the experimental results.

Park et al. [36] studied the electronic structure and magnetic properties of a macroscopic $Ge_{1-x}Mn_x$ crystal by the density functional method. It was shown that there are two channels of exchange between two dopant Mn^{2+} ions: direct antiferromagnetic exchange between neighboring ions (at sufficiently high manganese concentrations) and dominating indirect

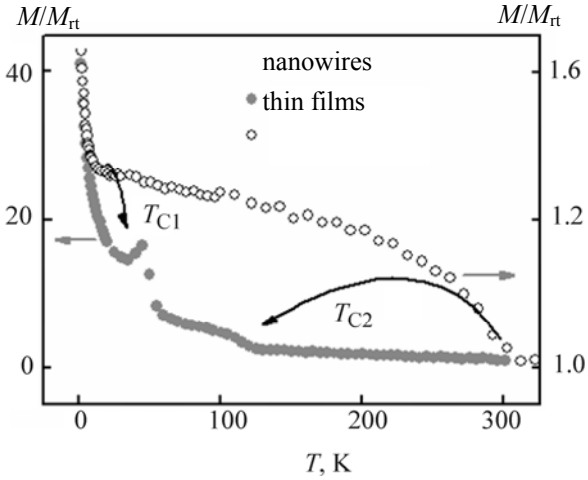

Fig. 2. Temperature dependences of the magnetic moment *M*, normed by the room-temperature magnetic moment M_{rt}, of $Ge_{1-x}Mn_x$ polycrystalline nanowires and thin films with the same dopant compositions. Magnetic field strength 1 kOe. Arrows show shifts of the Curie temperatures.

ferromagnetic exchange. The Curie temperatures were calculated by the percolation equation [39]:

$$kT_C = S(S + 1)J(R_{perc}),$$

where *k* is the Boltzman's constant; *S,* manganese ion spin; $J(R_{perc})$, exchange integral for two magnetic dopant ions separated by the percolation radius R_{perc} proportional to the mean interionic distance.

The calculated Curie temperature for a crystal is 300 K (at the manganese atomic fraction *x* of 2%). At the same time, the Curie temperature for $Ge_{0.98}Mn_{0.02}$ thin films is much lower (16 K) than predicted by the theory and that for $Ge_{0.99}Mn_{0.01}$ nanowires is higher (320 K) [11–14].

Thus, at present there is no universal theory capable of explaining the nature of ferromagnetism in different types of DMS. At the same time, preliminary experimemnts [11–14] show that a transition to nanosizes can much improve the properties of DMS. Figure 2 presents the temperature dependences of magnetic moment for $Ge_{1-x}Mn_x$ thin films and nanowires with the same dopant composition. As seen, size limitation of the $Ge_{1-x}Mn_x$ system leads to a change of the T_{C1} and T_{C2}, temperatures for dispersed Mn^{2+} ions and GeMn clusters, respectively. In going from thin films to nanowires, T_{C1} increases from 16 K to 35 K and T_{C2}, by contrast, decreases from 285 K to 125 K, which is probably associated with decreased size of GeMn clusters.

Specifics of Static and High-Frequency Dymanic Magnetic Properties of Nanowires

There are general regularities in the magnetic properties of ferromagnetic nanowires, irrespective of the material they are made of. There regularities are underlain by the quasi-one-dimensionality of nanowires and their strong shape anisotropy. Below we consider the main properties of composition materials containing ferromagnetic nanowires and their difference from macroscopic materials.

It was established [41, 42] that the ratio of the diameter to mean interwire spacing much affects the coercivity and magnetic anisotropy of nanowires. The anisotropy field tends to arrange the nanowire magnetization vectors uniformly along the easy magnetization axes in mutually opposite directions so that to reduce the saturation magnetization M_s and, as a result, total energy of nanowires. The effective anisotropy field depens on the surface, magnetocrystallic, and magnetoelastic contributions. The effective ansotropy field in nanowires is most contributed by the surface anisotropy. Thus, the nanowire anisotropy field is determined by two competing contributions [43, 44]:

$$H_a = 2\pi M_s - 6\pi M_s f,$$

where the first term relates to the surface anisotropy, the second relates to dipole–dipole coupling of nonowires, and f is the shape and filling factor.

The f factor is calculated by the formula:

$$f = \frac{\pi}{2\sqrt{3}} (d/D)^2,$$

where d is the nanowire diameter, and D, mean interwire spacing.

Note that the f factor determined the magnetic size of the nanowire assembly: $f = 0$ ($H_a = 2\pi M_s$) is characteristic of isolated cylindrical nanowires, $f = 1$ ($H_a = -4\pi M_s f$) is characteristic of a thin long nanowire assembly with magnetically similar nanowires. In the nanowire assembly in anodized aluminamembrane pores, the f factor takes intermediate values, which is indicative of magnetic size effects of this nanocomposite.

The nanowire shape anisotropy affects spin dynamics in high-frequency magnetic fields. The magnetic behavior of nanowires is determined by collective spin modes. Figure 3a schematically depicts several modes with a nonzero component perpendicular to a "thick" nanowire axis [45]. In "thin" nanowires, the perpendicular mode is almost suppressed because of the small nanowire diameter. Spin–wave excitations propagate exclusively along the nanowire axis (Fig. 3b). In the case of structural disorder (for example, polycrystallinity), these spin–wave modes can be localized (Fig. 3c) [46], which restricts spin–wave propagations along the nanowire, too. The above modes determine the spin dinamics in nanowires in high-frequency magnetic fields and affect the electron spin resonance spectra. Actually, the axial spin waves have a short wave vector (shorter than $1/L$, where L is the nanowire length). By contrast, the radial waves have a long wave vector inversely related to the nanowire diameter, an the corresponding resonance frequencies fall in the infrared range (nanowire diameter ~1–10 nm). Thus, the spin dynamics in nanowires allows separation of the axial a radial components of spin waves, which is impossible with macroscopic materials.

One more feature differentiating ferromagnetic nanowires from macroscopic solids cosists in the following. As known, the contribution of dipole–dipole spin coupling in macroscopic ferromagnetic materials is negligibly low compared with the contribution of exchange spin coupling. At the same time, it was showm theoretically [47] that in nanowires of the diameter $d < d_c = D_{ex}\sqrt{(D_{ex}\pi/M_s)}$ is the exchange constant) the contributions of dipole–dipole and exchange spin coupling compare with each other, because the dipole–dipole spin coupling in quasi-one-dimensional nanowires is much contributed by not only the nearest neighboring atoms, but also farther neighbors. In other words, the spin wave modes contain two components: dipole and exchange. The calculated ferromagnetic resonance spectrum (Fig. 4) of ferromagnetic nanowires with $d < d_c$ shows two maxima, one corresponding to the "exchange" mode and the other to "dipole" modes [47].

Thus, there are certain specific features in the spin dynamics of nanowires, which differentiates the latter from nanofilms and macroscopic samples.

Nanowires on the Basis of Ferromagnetic Oxides and $A^{II}B^{VI}$ and $A^{III}B^{V}$ Semiconductors

Nanowires of optically transparent semiconductor materials of Group II and VI elements, such as CdS, CdSe, and ZnS, are fairly well studied owing to their unique optical properties. As expected, doping such nanowires with transition metals would allow controlling their luminescence by means of magnetic field. The first nanowires doped with trasition metals

were reported by Chen et al. [48]. These nanowires were synthesized in MSM-41 silica pores. Studying the magnetic properties of manganese-doped nanowires of the composition $Cd_{1-x}Mn_xS$ [48] established that these nanowire are paramagnetic, when the manganese dopant concentration x is below 0.2. At $0.2 < x < 0.8$ they are spin glass-like (frozen randomly oriented spins). Macroscopic samples of the same composition with $x > 0.8$ exhibit long-range antiferro-magnetic ordering which is suppressed in nanowires in view of the known instability of long-range magnetic order in a one-dimensional system. Na et al. [49] synthesized $Cd_{1-x}Mn_xS$ nanowires by chemical vapor deposition (CVD) and demonstrated for the first time the possibility of controlling the optical properties of these nanowires by means of an external magnetic field.

Spintronic applications require DMS materials with a long spin coherence time (> 10 ns). This criterion is met by ZnO whose spin coherence time is 20 ns at room temperature [50]. At present metal oxide nanowires doped with Mn [51], Co [52], and Ni [52] have been synthesized. The synthesis of *p*- and *n*-type DMS nanowires on the basis of $Zn_{1-x}M_xO$ (M = Mn, Co, Ni) opens up the possibility for developing a dipolar spintronic transistor. The feasibilty of such transistors is evidenced by the ferromagnetism of $Zn_{1-x}M_xO$ nanowires grown by CVD [51, 53], associated with indirect coupling due to spin transfer with delocalized charge carriers: holes [54] and electrons [55]. The magnetic properties of these materials are of particular interest. For example, manganese-doped ZnO nanowires doped have the Curie temperature of 37–44 K [51, 53], whereas cobalt and nickel doping induce ferromagnetism at room temperature [52, 56]. Such a seemingly strange behavior can be explained, first, by that $Zn_{1-x}Mn_xO$ and $Zn_{1-x}Co_xO$ nanowires were grown by different procedures and, second, by that the doping admixtures have different electronic configurations: d^5 (Mn^{2+}) and d^7 (Co^{2+}), which, in its turn, can affect the Curie temperature. As shown in [57–59], cobalt-doped TiO_2 nanowires and $ZnO/Zn_{1-x}Co_xO$ core/shell nanocables can be used to develop a spin field effect transistor (spin-FET).

Zener calculations of the Curie temperature for a macroscopic $Ga_{1-x}Mn_xN$ crystal predicted $T_C \sim 300$ K [29]. The experimental Curie temperature of $Ga_{1-x}Mn_xN$ thin films, too, are fairly high, namely 250–370 K [60]. Generally, DMS systems of the $A^{III}B^{V}$ type are well studied both theoretically and experimentally. At the same time, no information on nanowires of these materials have still been reported. The first $Ga_{1-x}Mn_xN$ nanowires were reported by Deepak et al. [61], who established their Curie temperature (325 K), and it proved to be consistent both with the theoretical and experimental data for macroscopic materials and thin films of the same composition.

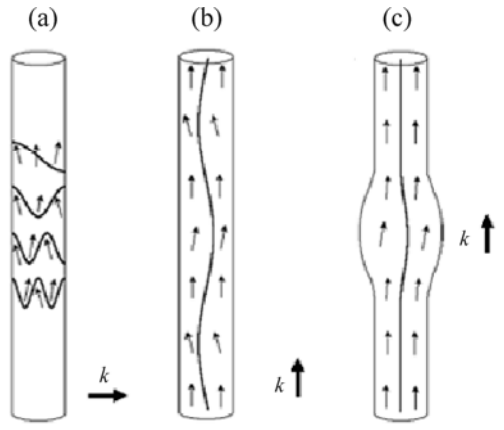

Fig. 3. Spin–wave modes in nanowires [45]: (a) wave vector k is perpendicular to the nanowire axis; (b) wave vector is parallel to the nanowire axis, and (c) localized mode.

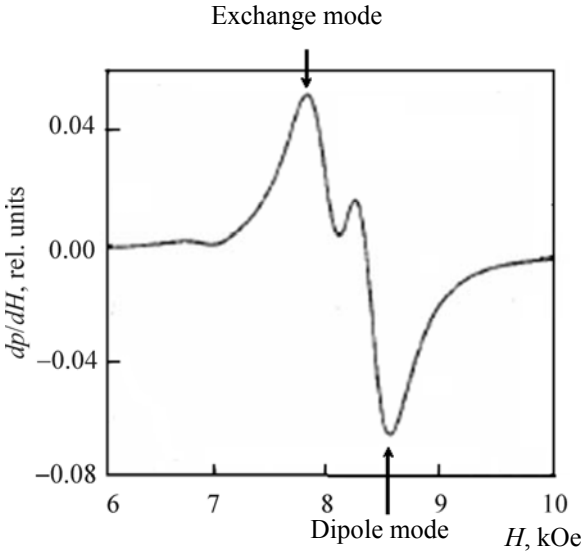

Fig. 4. Calculated ferromagnetic resonance spectrum (dependence of the field derivative of the absorbed microwave power P on the magnetic field strength H) for nickel nanowires 80 nm in diameter [47].

The magnetic and magnetotransport properties of CVD-grown $Ga_{1-x}Mn_xN$ nanowires with varied diameter, 10–100 nm, and a 7% manganese content. The coercive force measured by a SQUID magnetometer decreases with increasing temperature from 80 Oe at 5 K to 40 Oe at 300 K. Furthermore, $Ga_{1-x}Mn_xN$ nanowires show a negative magnetoresistance of 1.4% at 2 K and 0.4% at 250 K in an external magnetic field of 9 T. Such magnetic resistance is characteristic of $Ga_{1-x}Mn_xN$ thin films [63, 65]. Note that the coercive forces in nanowires of the same diamter and composition, measured in [60] and [62–64], differ considerably. This fact can be explained by different conditions of growing of these nanowires, say, by different temperature conitions. Furthermore, dopant clusters whose growth is difficult to control can also contribute much. Unfortunately, this contribution is not discussed or taken into account in the cited works. We beleive that the high-temperature ferromagnetism observed in most of these works is readily explained in terms of cluster ferromagnetism. The effect of synthesis conditions was also reported for $Ga_{1-x}Mn_xAs$ thin films [66].

Research on the magnetic and magnetotransport properties of CVD-grown $Ga_{1-x}Mn_xP$ nanowires showed that these materials are magnetically rigid ferromagnetics with T_C = 330 K, whereas the Curie temperature theoretically predicted for macroscopic samples of the same composition is 100 K. Moreover, $Ga_{1-x}Mn_xP$ nanowires exhibit a negative magnetoresistance of about 5%, while that measured in $Ga_{1-x}Mn_xP$ thin films is lower by an order of magnitude (0.35%). These values provide direct evidence for the particle size effect on the magnetic and magneto-transport properties of DMS materials of the $A^{III}B^{V}$ system. These materials were already used for creating prototype spin-FET devices and light-emitting diodes (spin-LED) for spintronics [62].

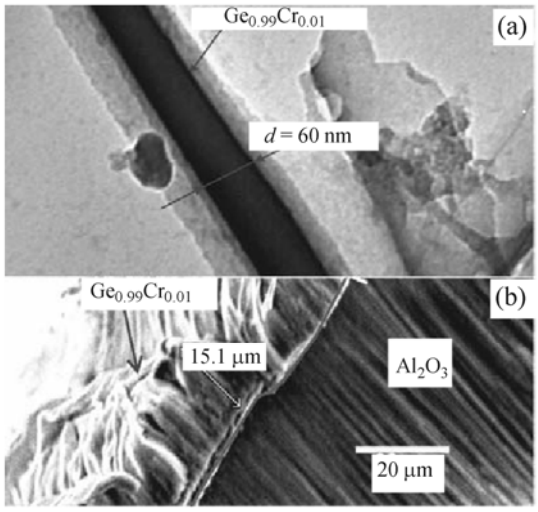

Fig. 5. Microphotographs of nanowires: (a) individual $Ge_{0.99}Cr_{0.01}$ nanowire; (b) ordered ensemble of $Ge_{0.99}Cr_{0.01}$ nanowires in an anodized Al_2O_3 membrane.

Nanowires on the Basis of Ferromagnetic Semiconductor Materials of Group IV Elements

Unlike DMS nanowires of the $A^{II}B^{VI}$ and $A^{III}B^{V}$ systems, DMS nanowires of Group IV elements have scarcely been reported. This looks quite strange, since silicon is a base of modern electronics and Group IV element nanowires can readily be integrated in modern electronic systems.

The synthesis and study of DMS nanowires of Group IV elements (Fig. 5) were first reported by the National Physical Laboratory (United Kingdom, Teddington) and University College Cork (Ireland, Cork). The nanowires were grown using supercritical CO_2 [67]. This method of growing nanowires has a number of advantages. First, the nanowire growth process is as little as 15–30 min long, whereas other syntheses take a few days. Second, having high diffusion coefficients in a low-viscosity supercritical fluid, reagent molecules readily penetrate into nanopores of the medium where nanowires are grown. The anodized alumina membranes used for such a medium allowed production of oriented nanowires with readily controlled and reliably reproduced diameter, lenth, and mean interparticle spacings. The starting reagent was diphenyl germanite mixed with manganese dicabonyl (synthesis of $Ge_{1-x}Mn_x$ nanowires), dicobalt octacarbonyl ($Ge_{1-x}Co_x$ nanowires), and chromium dicarbonyl ($Ge_{1-x}Cr_x$ nanowires); the atomic fraction of transition metal dopants in the nanowires varied from 1 to 5%. The nanowire diameters were 35, 50, and 60 nm, and the mean spacings between separate nanowires were 200 and 300 nm. The structural and chemical characteristics of nanowires were studied by means of trasmission electron microscopy, X-ray diffraction, X-ray photoelectron spectroscopy, and XANES (X-ray absorption near edge structure) spectroscopy.

Nanowires of $Ge_{0.99}Mn_{0.01}$ consist of a polycrystalline germanium doped with Mn^{2+} and Mn^{3+}. The Mn^{3+} and Mn^{2+} groups are spacially separated: Mn^{3+} ions locate closer to the nanowire center, while Mn^{2+}

ions are closer to the surface. Furthermore, it was found that Mn does not form coarse clusters, and no Ge_8Mn_{11}, Ge_5Mn_3, and Ge_3Mn_5 magnetic alloys were detected in the nanowires [68].

Measurement of field dependences revealed a hysteresis of the magnetic moment of nanowires already at room temperature, implying magnetic ordering (Fig. 6) [11–14]. The Curie temperature of $Ge_{0.99}Mn_{0.01}$ nanowires is 320 K. This is the highest Curie temperature for a ferromagnetic in a series of materials (thin films and macroscopic semiconductors) with the same dopant composition. The theoretical models including indirect exchange coupling of localized spins and delocalized charge carrier spins and using ab initio calculations [29] predict much lower Curie temperatures than that of $Ge_{0,99}Mn_{0,01}$ nanowires. However, as shown above, the Curie tem-perature for a $Ge_{1-x}Mn_x$ diluted magnetic semicon-ductors, calculated in [36] in the framework of the DFT and percolation approximation, is 300 K (for x = 2%), which the experimental T_C for $Ge_{0.98}Mn_{0.02}$ thin films, obtained in the same work, is much lower.

Thus, at present there is no consistent theory to explain the nature of the ferromagnetism of Group IV-based DMS materials and the high Curie temperature of quasi-one-dimensional $Ge_{0.99}Mn_{0.01}$ nanowires.

Studies on the high-frequency magnetic and electroconducting properties of $Ge_{0.99}Mn_{0.01}$ nanowires [12–14] showed that the ESR spectrum (Fig. 7) contains lines of localized manganese ions and delocalized charge carriers. Analysis of the orientation dependences of ferromagnetic resonance made it possible to determine the nanowire anisotropy field (H_a = 30 Oe) and to establish that the nanowire axis is an easy magnetization axis. The absolute specific microwave electroresistance of the nanowires, determine from the ESR spectrun of charge carriers, proved to equal 10^{-3} Ω cm at 4 K, which is close to the specific resistance of germanium doped with transition metals (1%), measured by other methods [69].

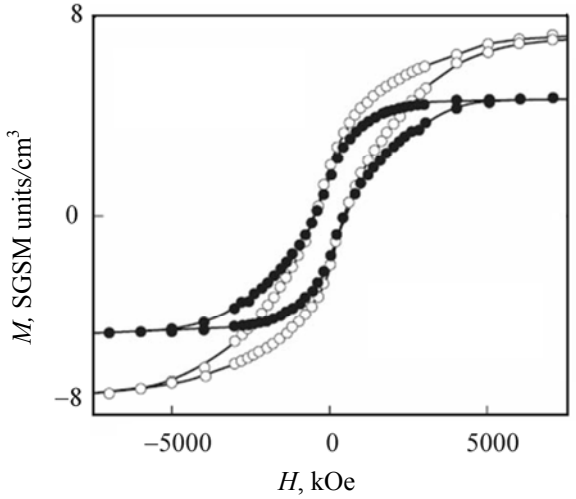

Fig. 6. Magnetic hysteresis loops of oriented $Ge_{0.99}Mn_{0.01}$ nanowires (diameter 60 nm) at (black circles) 300 K and (light circles) 1.8 K [11].

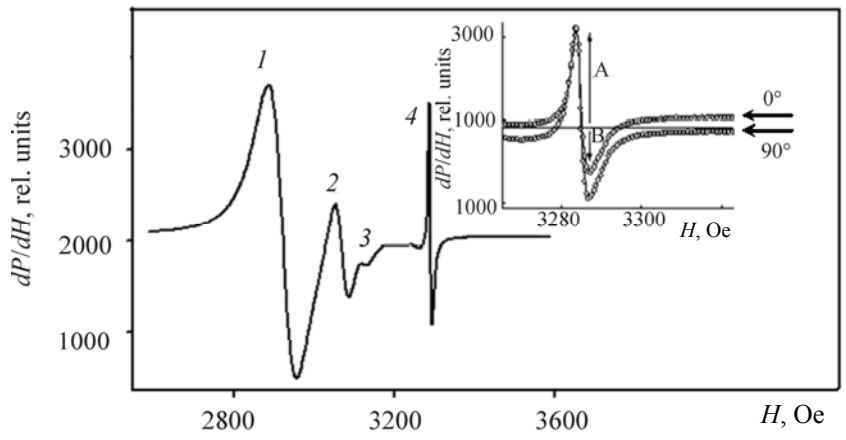

Fig. 7. ESR spectrum (dependence of the field derivative of the absorbed microwave power P on the magnetic field strength H) of $Ge_{0.99}Mn_{0.01}$ nanowires (diameter 60 nm) at the spectrometer magnetic field applied along the nanowire axis. (*1*, *2*, *3*, *4*) Spectral lines. (Insert) Asymmetric Dawson line 4 at the angles 0° and 90° between the nanowire axis and constant magnetic field of the spectrometer. Sample temperature 15 K. Amplitudes of the (A) downfield and (B) upfield wings of the Dawson line.

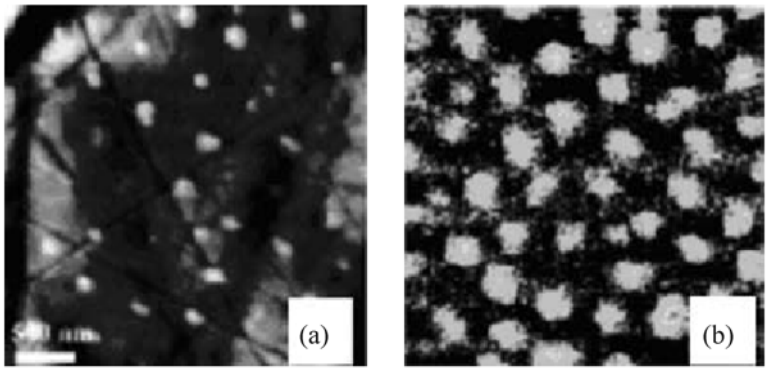

Fig. 8. ASM images of (a) polished sufrace of GeMn nanowires in an anodized alumina membrane and (b) current map. (View along the nanowire axis). The current reliefs were registered using an atomic force microscope with an electroconductivity measurement unit [70].

Kulkarni et al. [70] could measure the specific electroconductivity of separate nanowires at constant current. The microphotographs in Fig. 8 demonstrate the topography of a polished surface and curent reliefs of the nanowire assembly surface, obtained at 20 and 40 V (the photographs were obtained with an atomic force microscope). The specific electroconductivity of individual nanowires proved to be much higher than the electroresistance of bulk materials of the same composition, which the authors explained by effective scattering of charge carriers with nanowire surface.

Thin Films of Ferromagnetic Semiconductor Materials

At present a huge number of publication have been devoted to DMS thin films (for example, see [71–77]). However, a lot of problems are still to be solved, among them the problem of size dependence of magnetoresistance in Ge:Mn nanostructures (to solve this problem, one should compare the marnetotransport effects in quasi-one-dimensional nanowires and quasi-two-dimwnsional thin films).

Ferromagnetic resonance and spin wave resonance in thin ferromagnetic films. One of the key properties of DMS thin films is magnetic anisotropy which plays an important role in the development of spintronic devices. Since the ferromagnetic order in DMS is associated with free charge carriers, the magnetic anisotropy of thin films should depend in part by the Fermi surface anisotropy [78].

Ferromagnetic resonance (FMR) is one of the most powerful tools for research on ferromagnetic thin films [79–86]. This method is useful to study their magnetic anisotropy, magnetic susceptibility, Curie temperature, and relaxation processes.

Along with the resonance mode with the wave vector $k = 0$, observed under uniform FMR, spin waves with a nonzero wave vector k can be excited in thin films. Analysis of the spin wave resonance spectra allows one to assess the exhange coupling between localized magnetic dopant ions, since the resonance frequency of the spin mode is proportional to the resonance line number: $H_{res} \sim Dn^a$ (D is the exchange stiffness constant; n, number of the resonance lines in the spin wave resonance spectrum, proportional to the wave vector of the spin wave mode; $a = 2$, in the case of a classical Kittel spin coating of a surface with a uniform thin film due to surface anisotropy forces). This allows determination of the exchange integral J and the energy of spin coupling between a transition metal dopant and a polarized charge carrier in magnetic semiconductors

$$J = Dg\mu_B/(2Sr_s^2),$$

where g is the g factor; μ_B, Bohr magneton; S, dopant spin; and r_s, spin–spin distance.

In the case of spin–wave resonance in nonuniform DMS thin films the, the exponent a may differ from the "classical" value of 2. For example, Sasaki et al. [90] reported a linear ($a = 1$) dependence of H_{res} on mode number ($H_{res} \sim n$), whereas Hoekstra et al. [86] observed a resonance with $H_{res} \sim n^{2/3}$.

Magnetoresistance in ferromagnetic semiconductors. All conductors possess higher or lower magneto-resistance. In metals this effect is only slightly pronounced. The relative magnetoresistance in semicon-

ductors can vary 100–10000 times more than in metals, reaching hundreds thousands percent.

Semiconuctors can exhibit a negative magnetoresistance [95, 96], for example, it was observed in (MnGa)As thin films [97, 98]. The negative magnetoresistance can be of different origin: spin-dependent scattering of charge carriers on alloy clusters formed on doping [99] or strong charge carrier–cluster dipole coupling, like that observed in a $Ga_{1-x}Mn_xAs$ sample containing MnAs clusters [100].

At high temperatures, current is associated with charge carriers thermally excited into the conduction band (so-called band conduction mechanism). At low temperatures, a dominating role in charge carrier transport may belong to hopping conduction. In this case, upon phonon absorption or emission, charge carriers move ("hop") over states localized at a high density in a certain energy range in the forbidden band of the material. The CC hopping conduction is associated with carriers localized on magnetic impurities.

According to the Shklovskii–Efros magnetoresistance model [101], the dependence of the relative in specific electroresistance on magnetic field is described by the function $\Delta\rho/\rho \sim \exp(-AH^2)$. This model nicely describes the negative magnetoresistance which, for example, was observed in a two-dimensional array of Ge/Si quantum dots [102]. In amorphous semiconductors with low dopant concentrations, the negative magnetoresistance can be caused by the follwing mechanism. The hopping electroconduction in amorphous semiconductors with low dopant concentrations are associated with charge carriers at the localized band tail states of the Fermi level [103, 104]. These localized states are degenerate in a zero magnetic field. Applied external magnetic field induces Zeeman splitting of the states. As a consequence, the hopping probability (and its proportional mobility of charge carriers) changes, like the density of states.

As a rule, both negative and positive magnetoresistance are observed in experiments [103, 104]. The former is observed in low magnetic fields and the latter at higher magnetic fields.

Spin dynamics and microwave magnetoresistance of manganese-implanted germanium this films. Veinger et al. [105–108] suggested a contactless procedure for measuring microwave (MW) magnetoresistance by means of ESR spectroscopy. The microwave magnetoresistance shows certain specific features compared with the constant current (CC) magnetoresistance. These features are associated with the skin effect which prevents microwave field penetration into a bulk sample.

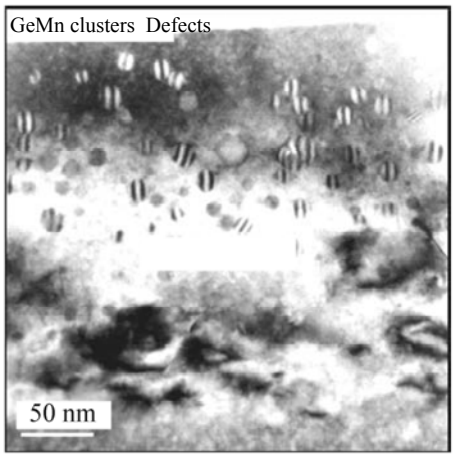

Fig. 9. Microphotograph of an ion-implanted Ge:Mn film (x = 4%).

The authors of the review made use of the procedure in [105–108] to measure the magnetoresistance of manganese-implanted germanium thin films (Fig. 9). Previously the magnetoresistance of $Ge_{1-x}Mn_x$ films was measured only in the CC mode [109–111]. The wave resistance of the MW tract in our used spectrometer is $R_g \approx 250\ \Omega$, which is a fortiori lower than that of $Ge_{1-x}Mn_x$ thin films. Therewith, the field derivative of the absorbed MW power dP/dH is proportional to the field derivative of magnetoresistance dR/dH.

It was shown by ESR spectroscopy [112–114] that the resonance absorption in $Ge_{1-x}Mn_x$ thin films at high temperatures ($T > 260$ K) is associated with the ferromagnetic resonance in GeMn alloy clusters, whereas the resonance at ($T < 60$ K) is induced by collective spin excitation in the crystal lattice of a sample. The temperature dependence of magnetic moment, obtained by means of a SQUID magnetometer, revealed critical temperatures corresponding magnetic ordering in clusters and in thin films.

The MW magnetoresistance in Ge:Mn thin films includes several components: Loretz magnetoreistance typical of two-dimensional systems [100], magnetoresistance due to spin splitting of charge carriers located near the Fermi level [103, 104], and anisotropic magnetoresistance due to spin-dependent

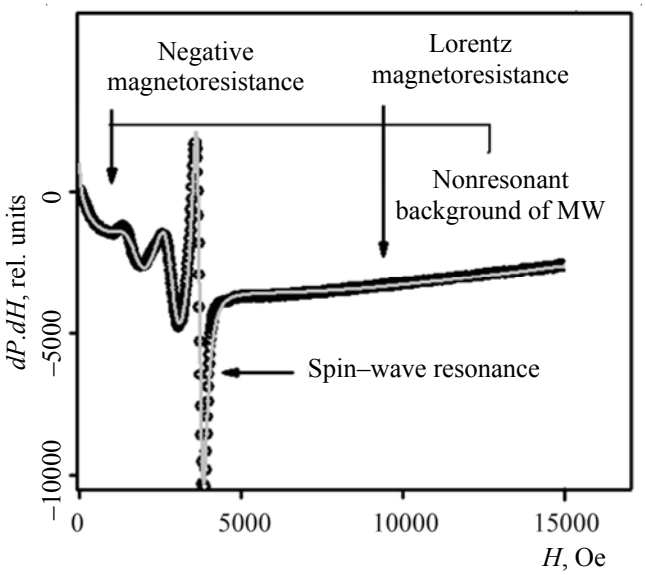

Fig. 10. Ferromagnetic resonance spectrum(dependence of the field derivative of the absorbed microwave power P on the magnetic field strength H) of a Ge:Mn thin film (x = 4%) at T = 262 K. Magnetic field is applied parallel to the film. The solid line shows the spectrum fitted by four Loretzian lines and a nonlinear magnetoresistance signal

scattering of charge carries from magnetic impurities [115] (Fig. 10).

Comparison of the MW absorption spectra of thin films with those of nanowires shows that size limitation results in complete suppression of MW magnetoresistance and strongly affects the ESR spectra of nanowires.

Even though ESR offers essential advantages for magnetic studies on DMS, the most part of published results for $Ge_{1-x}Mn_x$ thin films and macrocrystals were obtained in static conditions. Cho et al. [116, 117] reported the magnetic properties of $Ge_{1-x}Mn_x$ macrocrystals (x = 0.1–17.6%) grown by the Chokhralsky procedure.

The temperature dependence of magnetic moment for a $Ge_{1-x}Mn_x$ single crystal shows two critical points at ~290 and ~150 K, corresponding to Ge_3Mn_5 and Ge_8Mn_{11} clusters, respectively. At the same time, it is known that the temperature of long-range ferromagnetic ordering for a system of "dissolved" manganese ions whose exchange coupling occurs due to spin-polarized charge carriers is much lower, T_C = 16 K [118, 119]. This critical temperature was not observed in [116, 117], even though the dopant concentrations are fairly high. This is explained by the fact that the Chokhralsky procedure, unlike the above-described nanostructure growth procedures, is unsuitable for DMS, since the overwhelming part of the dopant form alloy aggregates.

Growing doped semiconductor nanostructures not always results in DMS formation. Thus, Li et al. [120] studied the magnetic and magnetotransport properties of $Ge_{1-x}Mn_x$ thin films (x = 25–42%) synthesized by molecular beam epitaxy. Even though the dopant concentration was quite high, the synthesized thin films did not pass into the ferromagnetic state at low temperatures. At temperatures below 20 K, the samples behaved as a spin glass. The other critical temperature (~150 K) correspoded to ferromagnetic ordering in Ge_8Mn_{11} clusters.

CONCLUSIONS

The comparison of diluted magnetic semiconductors with other candidate materials for spintronics applications, made in the present review, showed that the former hold the greatest promise.

At present a procedure for preparing nanocomposites containing assemblies of ordered semiconductor ferromagnetic nanowires in anodized alumina membranes has been developed. This is the first procedure which allows growing oriented nanowires with readily controlled and reliably reproduced lengths, diameters, and mean interwire spacings. Research into the magnetic properties of $Ge_{1-x}Mn_x$ nanowires showed that their Curie temperatures are much higher than those of macrocrystalline samples, and the nanowires themselves are prototype MRAM of a new generation.

ACKNOWLEDGMENTS

The work was financially supported by the Basic Research in Nanotechnologies and Nanomaterials Program of the Presidium of the Russian Academy of Sciences (no. 27).

REFERENCES

1. Baibich, M.N., Broto, J.M., Fert, A., et al., *Phys. Rev. Lett*., 1988, vol. 61, pp. 2472–2475.
2. Binasch, G., Grunberg, P., Saurenbach, F., and Zinn, W., *Phys. Rev. B*, 1989, vol. 39, pp. 4828–4830.
3. Camley, R.E. and Barnas, J., *Phys. Rev. Lett*., 1989, vol. 63, p. 664.
4. Barnas, J., Fuss, A., Camley, R.E., et al., *Phys. Rev. B*, 1990, vol. 42, pp. 8110–8120.

5. Barthelemy, A. and Fert, A., *Phys. Rev. B*, 1991, vol. 43, p. 13124.
6. Valet, T. and Fert, A., *Ibid*., 1993, vol. 48, pp. 7099–7113.
7. Butler, W. H., Zhang, X.-G., Schulthess, T. C., et al., *Ibid*., 1997, vol. 56, pp. 14574–14582.
8. Moodera, J.S., Kinder, L.R., Wong, T.M., and Meservey, R., *Phys. Rev. Lett*., 1995, vol. 74, pp. 3273–3276.
9. Hall, K.C. and Flatte, M.E., *Appl. Phys. Lett*., 2006, vol. 88, pp. 162503–162506.
10. Slaughter, J.M., Chen, E.Y., and Tehrani, S., *J. Appl. Phys*., 1999, vol. 85, pp. 4451–4453.
11. Kazakova, O., Kulkarni, J.S., Holmes, J. D., and Demokritov, S.O., *Phys. Rev*., 2005, vol. 72, pp. 094415–094421.
12. Morgunov, R.B., Dmitriev, A.I., Tanimoto, Y., and Kazakova, O.L., *J. Appl. Phys*., 2009, vol. 105, pp. 1215–1220.
13. Morgunov, R.B., Dmitriev, A.I., Tanimoto, Y., et al., *J. Magnetism Magnetic Mater*., 2007, vol. 310, issue 2, part 3, pp. 824–826.
14. Morgunov, R.B., Dmitriev, A.I., Tanimoto, Y., et al., *Fiz. Tverd. Tela*, 2007, vol. 49, no. 2, pp. 285–290.
15. Flatte, M. E. and Vignale, G., *Appl. Phys. Lett*., 2001, vol. 78, p. 1273.
16. Flatte, M.E., Yu, Z.G., Johnston-Halperin, E., and Awschalom, D.D., *Ibid*., 2003, vol. 82, pp. 4740–4742.
17. Tsoi, M., Jansen, A.G.M., Bass, J., et al., *Phys. Rev. Lett*., 1998, vol. 80, pp. 4281–4284.
18. Katine, J.A., Albert, F.J., Buhrman, R.A., et al., *Ibid*., 2000, vol. 84, pp. 3149–3152.
19. Kikkawa, J.M., Smorchkova, I.P., Samarth, N., and Awschalom, D.D., *Science*, 1997, vol. 277, pp. 1284–1287.
20. Kikkawa, J.M. and Awschalom, D.D., *Phys. Rev. Lett*., 1998, vol. 80, pp. 4313–4316.
21. Ney, A., Harris, J.S. Jr., and Parkin, S.S.P., *J. Phys.: Condens. Matter*, 2006, vol. 18, pp. 4397–4406.
22. Motsnyi, V.F., van Dorpe, P., van Roy, W., et al., *Phys. Rev. B*, 2003, vol. 68, pp. 245319–245332.
23. Wang, J., Knodaparast, G.A., Kono, J., et al., *J. Modern Optics*, 2004, vol. 51, pp. 2771–2728.
24. Sun, B., Jiang, D., Sun, Z., et al., *J. Appl. Phys*., 2006, vol. 100, pp. 083104–083109.
25. Ohno, H., Chiba, D., Matsukura, F., et al., *Nature,* 2000, vol. 408, pp. 944–946.
26. Chiba, D., Yamanouchi, M., Matsukura, F., and Ohno, H., *Science*, 2003, vol. 301, pp. 943–945.
27. Matsukura, F., Ohno, H., Shen, A., and Sugawara, Y., *Phys. Rev. B*, 1998, vol. 57, pp. 2037–2040.
28. Akai, H., *Phys. Rev. Lett*., 1998, vol. 81, pp. 3002–3005.
29. Dietl, T., Ohno, H., Matsukura, F., et al., *Science*, 2000, vol. 287, pp. 1019–1022.
30. Zener, C., *Phys. Rev*., 1951, vol. 82, pp. 403–405.
31. Yagi, M., Noba, K., and Kayanuma, Y., *J. Lumin*., 2001, vol. 94, pp. 523–527.
32. Edmonds, K.W., Bogusławski, P., Wang, K.Y., et al., *Phys. Rev. Lett*., 2004, vol. 92, pp. 037201–037203.
33. Ruderman, M. and Kittel, C., *Phys. Rev*., 1954, vol. 96, pp. 99–102.
34. Yosida, K., *Ibid*., 1957, vol. 106, pp. 893–898.
35. Zhao, Y.J., Shishido, T., and Freeman, A.J., *Phys. Rev. Lett*., 2003, vol. 90, pp. 047204–047208.
36. Park, Y. D., Hanbicki, A. T., Erwin, S.C., et al., *Science*, 2002, vol. 295, pp. 651–654.
37. Kim, Y., Cho, S., Choi, S.Y., et al., *Phys. Rev. B*, 2002, vol. 66, pp. 033303–033306.
38. Krstajic, P.M., Ivanov, V.A., Peeters, F.M., et al., *Europhys. Lett*., 2003, vol. 61, pp. 235–241.
39. Litvinov, V.I. and Dugaev, V.K., *Phys. Rev. Lett*., 2001, vol. 86, p. 5593.
40. Demand, M., Encinas-Oropesa, A., Kenane, S., et al., *J. Magnetism Magnetic Mater*., 2002, vol. 249, issue 2, part 3, pp. 228–233.
41. Ramos, C.A., Vasallo Brigneti, E., and Vazquez, M., *Physica B*, 2004, vol. 354, pp. 195–197.
42. Vazquez, M., Hernandez-Velez, M., Pirota, K., et al., *Eur. Phys. J., B*, 2004, vol. 40, pp. 489–497.
43. Encinas, A., Demand, M., Vila, L., et al., *Appl. Phys. Lett*., 2002, vol. 81, pp. 2032–2034.
44. Encinas-Oropesa, A., Demand, M., Piraux, L., et al., *Phys. Rev. B*., 2001, vol. 63, pp. 104415–104421.
45. Chipara, M.I., Skomski, R., and Sellmyer, D.J., *J. Magnetism Magnetic Mater*., 2002, vol. 249, issue 2, pp. 246–250.
46. Skomski, R., Zeng, H., Zheng, M., and Sellmyer, D.J., *Phys. Rev. B*., 2000, vol. 62, pp. 3900–104421.
47. Arias, R. and Mills, D.L., *Ibid*., 2001, vol. 63, pp. 134439–134450.
48. Chen, L., Klar, P.J., Heimbrodt, W., et al., *Appl. Phys. Lett*., 2001, vol. 76, pp. 3531–3533.
49. Na, C.W., Han, D.S., Kim, D.S., et al., *J. Phys. Chem. B*, 2006, vol. 110, pp. 6699–6704.
50. Ghosh, S., Sih, V., Lau, W. H., et al., *Appl. Phys. Lett*., 2005, vol. 86, pp. 232507–232510.
51. Chang, Y.Q., Wang, D.B., Luo, X.H., et al., *Ibid*., 2003, vol. 83, pp. 4020–4022.
52. Cui, J.B. and Gibson, U.J., *Ibid*., 2005, vol. 87, pp. 133108–133111.
53. Liu, J.J., Yu, M.H., and Zhou, W.L., *Ibid*., 2005, vol. 87, pp. 172505–172508.
54. Kittilstved, K.R., Norberg, N.S., and Gamelin, D.R., *Phys. Rev. Lett*., 2005, vol. 94, pp. 147209–147213.

55. Venkatesan, M., Fitzgerald, C.B., Lunney, J.G., and Coey, J.M.D., *Ibid*., 2004, vol. 93, pp. 177206–177210.
56. Cui, J. and Gibson, U.J., *J. Phys. Chem. B*, 2005, vol. 109, p. 22074.
57. Lee, Y.H., Yoo, J.M., Park, D.H., et al., *Appl. Phys. Lett*., 2005, vol. 86, pp. 033110–033113.
58. Greytak, A.B., Lauhon, L.J., Gudiksen, M.S., and Lieber, C.M., *Ibid*., 2004, vol. 84, pp. 4176–4178.
59. Han, S., Zhang, D., and Zhou, C., *Ibid*., 2006, vol. 88, p. 133109.
60. Reed, M.L., El-Masry, N.A., Stadelmaier, H.H., et al., *Ibid*., 2001, vol. 79, pp. 3473–3475.
61. Deepak, F.L., Vanitha, P.V., Govindaraj, A., and Rao, C.N.R., *Chem. Phys. Lett*., 2003, vol. 374, pp. 314–318.
62. Choi, H.J., Seong, H.K., Chang, J., et al., *Adv. Mater*., 2005, vol. 17, pp. 1351–1356.
63. Han, D.S., Park, J., Rhie, K.W., et al., *Appl. Phys. Lett*., 2005, vol. 86, pp. 032506–032509.
64. Shon, Y., Kwon, Y.H., Kang, T.W., et al., *J. Cryst. Growth*, 2002, vol. 245, pp. 193–197.
65. Sardar, K., Raju, A.R., Bansal, B., et al., *Solid State Commun*., 2003, vol. 125, pp. 55–57.
66. Park, Y.D., Lim, J.D., Suh, K.S., et al., *Phys. Rev. B*, 2003, vol. 68, pp. 085210–085215.
67. Holmes, J.D., Lyons, D.M., and Ziegler, K.J., *J. Chem. Eur*., 2003, vol. 9, pp. 2144–2150.
68. Kulkarni, J.S., Kazakova, O., Erts, D., et al., *Chem. Mater*., 2005, vol. 17, p. 3615.
69. Li, A.P., Wendelken, J.F., Shen, J., et al., *Phys. Rev. B*, 2005, vol. 72, pp. 195205–195214.
70. Erts, D., Polyakov, B., Daly, B., et al., *J. Phys. Chem. B*, 2006, vol. 110, pp. 820–826.
71. Kimel, A.V., Astakhov, G.V., Schott, G.M., et al., *Phys. Rev. Lett*., 2004, vol. 92, pp. 237203–237207.
72. Mitsumori, Y., Oiwa, A., Slupinski, T., et al., *Phys. Rev. B*, 2004, vol. 69, pp. 033203–033207.
73. Liu, X., Zhou, Y.Y., and Furdyna, J.K., *Ibid*., 2007, vol. 75, pp. 195220–195228.
74. Rappoport, T.G., Redlinski, P., Liu, X., et al., *Ibid*., 2004, vol. 69, pp. 125213–125224.
75. Goennenwein, S.T.B., Graf, T., Wassner, T., et al., *Appl. Phys. Lett*., 2003, vol. 82, pp. 730–732.
76. Sato, K., Fukushima, T., and Katayama-Yoshida, H., *Jpn. J. Appl. Phys*., 2007, vol. 46, pp. 628–684.
77. Liu, X. and Furdyna, J. K., *J. Phys.: Condens. Matter*, 2006, vol. 18, p. 245.
78. Abolfath, M., Jungwirth, T., Brum, J., and MacDonald, A.H., *Phys. Rev. B*, 2001, vol. 63, pp. 054418–054432.
79. Farle, M., *Rep. Prog. Phys*., 1998, vol. 61, pp. 755–793.
80. Nojiri, H., Motokawa, M., Takeyama, S., et al., *Physica B*, 1998, vol. 256, pp. 569–572.
81. Sasaki, Y., Liu, X., Furdyna, J.K., et al., *J. Appl. Phys*., 2002, vol. 91, pp. 7484–7486.
82. Goennenwein, S.T.B., Graf, T., Wassner, T., et al., *J. Supercond*., 2003, vol. 16, pp. 75–78.
83. Liu, X., Sasaki, Y., and Furdyna, J.K., *Phys. Rev. B*, 2003, vol. 67, pp. 205204–205213.
84. Dziatkowski, K., Palczewska, M., Słupinski, T., and Twardowski, A., *Phys. Rev. B*, 2004, vol. 70, pp. 115202–115214.
85. Liu, X., Lim, W.L., Ge, Z., et al., *Appl. Phys. Lett*., 2005, vol. 86, pp. 112512–112515.
86. Hoekstra, B., Stapele, R.P., and Robertson, J.M., *J. Appl. Phys*., 1977, vol. 48, pp. 382–395.
87. Bouzerar, G. and Pareek, T., *Phys. Rev. B*, 2002, vol. 65, p. 153203.
88. Omiya, T., Matsukura, F., Dietl, T., et al., *Physica E*, 2000, vol. 7, pp. 976–980.
89. Kittel, C., *Phys. Rev*., 1958, vol. 110, pp. 1295–1297.
90. Sasaki, Y., Liu, X., and Furdyna, J. K., *J. Supercond*., 2003, vol. 16, pp. 143–145.
91. Goennenwein, S.T.B., Wassner, T. A., Huebl, H., et al., *Appl. Phys. Lett*., 2003, vol. 82, pp. 730–732.
92. Tremblay, F., Pepper, M., Ritchie, D., et al., *Phys. Rev. B*, 1989, vol. 39, pp. 8059–8061.
93. Tremblay, F., Pepper, M., Newbury, R., et al., *Ibid*., 1989, vol. 40, pp. 10052–10055.
94. Roy, A., Levy, M., Guo, X.M., et al., *Ibid*., 1989, vol. 39, pp. 10185–10191.
95. Zhang, Y., Dai, P., Levy, M., and Sarachik, M.P., *Phys. Rev. Lett*., 1990, vol. 64, pp. 2687–2690.
96. Parish, M.M. and Littlewood, P.B., *Nature,* 2003, vol. 426, pp. 162–165.
97. Iye, Y., Oiwa, A., Endo, A., et al., *Mat. Sci. Eng. B*., 1999, vol. 63, pp. 88–95.
98. Ohno, H., Munekata, H., Penney, T., et al., *Phys. Rev. Lett*., 1992, vol. 68, pp. 2664–2667.
99. Wellmann, P.J., Garcia, J.M., Feng, J.L., and Petroff, P.M., *Appl. Phys. Lett*., 1997, vol. 71, pp. 2532–2534.
100. Akinaga, H., Boeck, J., Borghs, G., et al., *Ibid*., 1998, vol. 72, pp. 3368–3370.
101. Shklovskii, B.I. and Spivak, B.Z., *Hopping Transport in Solids*, Pollak, M. and Shklovskii, B., Eds., Amsterdam: Elsevier, 1991, p. 271.
102. Yakimov, A.I., Dvurechenskii, A.V., Minkov, G.M., et al., *Phys. Status Solidi C*, 2006, vol. 2, pp. 296–299.
103. Kubelik, I. and Triska, A., *Czech. J. Phys. B*, 1973, vol. 23, pp. 123–129.
104. Khosla, R.P. and Fischer, J.R., *Phys. Rev. B*, 1970, vol. 2, pp. 4084–4097.

105. Veinger, A.I., Zabrodskii, A.G., Tisnek, T.V., and Biskupski, G., *Fiz. Tekh. Poluprovod*., 1998, vol. 32, no. 5, pp. 557–563.
106. Veinger, A.I., Zabrodskii, A.G., and Tisnek, T.V., *Ibid*., 2000, vol. 34, no. 7, pp. 774–782.
107. Veinger, A.I., Zabrodskii, A.G., and Tisnek, T.V., *Ibid*., 2002, vol. 36, no. 7, pp. 826–835.
108. Veinger, A.I., Zabrodskii, A.G., and Tisnek, T.V., *Ibid*., 2005, vol. 36, no. 10, pp. 1159–1163.
109. Song, S.H., Lim, S.H., Jung, M.H., et al., *J. Korean Phys. Soc*., 2006, vol. 49, pp. 2386–2396.
110. Yu, S.S., Anh, T.T.L., Ihm, Y.E., et al., *Curr. Appl. Phys*., 2006, vol. 6, pp. 545–548.
111. Li, H., Wu, Y., Guo, Z., et al., *J. Appl. Phys*., 2006, vol. 100, p. 103908.
112. Morgunov, R., Farle, M., Passacantando, M., Ottaviano, L., and Kazakova, O., *Phys. Rev. B*, 2008, vol. 78, p. 045206.
113. Kazakova, O., Morgunov, R., Kulkarni, J., et al., *Ibid*., 2008, vol. 78, p. 235317.
114. Morgunov, R.B., Farle, M., and Kazakova, O.L., *Zh. Eksp. Teor. Fiz.,* 2008, vol. 134, pp. 141–155.
115. Wellmann, P.J., Garcia, J.M., Feng, J.L., and Petroff, P.M., *Appl. Phys. Lett*., 1997, vol. 71, pp. 2532–2534.
116. Cho, S.L., Choi, S.Y., Hong, S.C., et al., *Phys. Rev. B*, 2002, vol. 66, pp. 033303–03305.
117. Kim, S.K., Park, S.E., Cho, Y.C, et al., *J. Korean Phys. Soc*., 2006, vol. 49, pp. 518–522.
118. Panguluri, R.P., Nadgorny, B., Zeng, C., et al., Phys. *Status Solids*, 2005, vol. 242, pp. 67–50.
119. Bihler, C., Jaeger, C., Vallaitis, T., et al., *Appl. Phys. Lett*., 2006, vol. 88, pp. 112506–112509.
120. Li, H., Wu, Y., Guo, Z., et al., *J. Appl. Phys*., 2006, vol. 100, pp. 103908–103917.